Gluon saturation and baryon stopping in the SPS, RHIC, and LHC energy regions*

LI Shuang(李双)[1] FENG Sheng-Qin(冯笙琴)[1,2,3;1)]

[1] College of Science, China Three Gorges University, Yichang 443002, China
[2] Key Laboratory of Quark and Lepton Physics (Huazhong Normal University), Ministry of Education, Wuhan 430079, China
[3] School of Physics and Technology, Wuhan University, Wuhan 430072, China

Abstract: A new geometrical scaling method with a gluon saturation rapidity limit is proposed to study the gluon saturation feature of the central rapidity region of relativistic nuclear collisions. The net-baryon number is essentially transported by valence quarks that probe the saturation regime in the target by multiple scattering. We take advantage of the gluon saturation model with geometric scaling of the rapidity limit to investigate net baryon distributions, nuclear stopping power and gluon saturation features in the SPS and RHIC energy regions. Predictions for net-baryon rapidity distributions, mean rapidity loss and gluon saturation feature in central Pb+Pb collisions at the LHC are made in this paper.

Key words: gluon saturation, geometrical scaling, net-baryon distributions

PACS: 25.75.-q, 25.75.Ag, 25.75.Nq **DOI:** 10.1088/1674-1137/36/2/006

1 Introduction

During relativistic heavy-ion collisions, the fast valence quarks in one nucleus scatter in another nucleus by exchanging soft gluons, leading to their redistribution in rapidity space. The net-baryon number is essentially transported by valence quarks that probe the saturation regime in the target by multiple scattering.

Experimental heavy-ion investigations at the Large Hadron Collider (LHC) pay much more attention to the mid-rapidity region since ALICE covers rapidity up to $|y| = 2$. It provides measurements of lower x than before on an energy scale that is high enough to provide crucial tests of gluon saturation. Therefore the LHC will provide more opportunities to study the gluon saturation feature at small x.

At very high energies or small values of Bjorken variable x, the density of partons per unit transverse area, in a nucleon or nucleus becomes so large that it would lead to a gluon saturation of partonic distribution. The existence of this phenomenon was confirmed in experiments at HERA [1, 2]. Typical results from the experiments contain two parts: the small x problem and geometric scaling. It was predicted by an effective theory, CGC (Color Glass Condensate), which describes the behavior of the small x components of the hadronic wave function in QCD. In this paper, we use this CGC theory to discuss the questions of nuclear stopping and gluon saturation in relativistic heavy-ion collisions at SPS, RHIC and LHC.

The kinetic energy of the relativistic heavy-ion collisions that is removed from the beam and which is available for the production of a state such as the QGP (quark gluon plasma) depends on the amount of stopping between colliding ions. Stopping can be estimated from the rapidity loss experienced by baryons in the colliding nuclei [3–9]. If the incoming beam baryons have rapidity $y_{\rm b}$ relative to the CM (which has $y = 0$) and average rapidity

$$\langle y\rangle = \int_0^{y_{\rm b}} y{\rm d}y{\rm d}N/{\rm d}y \Big/ \int_0^{y_{\rm b}} {\rm d}y{\rm d}N/{\rm d}y, \qquad (1)$$

Received 9 May 2011

* Supported by National Natural Science Foundation of China (10975091), Excellent Youth Foundation of Hubei Scientific Committee (2006ABB036) and Education Commission of Hubei Province of China (Z20081302)

1) E-mail: fengsq@ctgu.edu.cn

the average rapidity loss is

$$\langle \delta y \rangle = y_{\rm b} - \langle y \rangle. \tag{2}$$

Here $\mathrm{d}N/\mathrm{d}y$ denotes the number of net-baryons (number of baryons minus the number of anti-baryons) per unit of rapidity. The studies of net baryon distributions and nuclear stopping have been discussed using a non-uniform collective flow model [10–13]. We will use gluon saturation to study net-baryon distributions in this paper.

Here we should mention a novel gluon saturation model proposed by Yacine Mehtar-Tani and Georg Wolschin [14, 15]. An analytical scaling law is derived within the color glass condensate framework based on small-coupling QCD in this model. Inspired by this model [14, 15], we study the net baryon distributions of central collisions in the SPS and RHIC energy regions by introducing the effective quark mass and rapidity limit of the gluon saturation region. Here we use a new geometric scaling method to define the rapidity limit of the gluon saturation region. The important difference is the definition of geometric scaling between our model and Ref. [14, 15]. It realized [14, 15] that geometric scaling is mainly about the peak positions of net-baryon rapidity distribution. But our model realizes the geometric scaling of net-baryon rapidity distribution is mainly about the gluon saturation rapidity limit. Net-baryon rapidity distributions and mean rapidity loss in central Pb+Pb collisions at the LHC are predicted in this paper.

2 Gluon saturation model with geometric scaling

Ideas for the color glass condensate are motivated by HERA data on the gluon distribution function [1]. Gluon density, $xG(x,Q^2)$, rises rapidly as a function of decreasing fractional momentum, x, or increasing resolution Q. This rise in gluon density ultimately owes its origin to the non-Abelian nature of QCD and that the gluons carry color charge. At higher and higher energies, smaller x and larger Q become kinematically accessible. A rapid rise with $\ln(1/x)$ was expected in a variety of theoretical works [14–23]. Due to the intrinsic non-linearity of QCD, gluon showers generate more gluon showers producing an exponential avalanche toward small x. The physical consequence of this exponential growth is that the density of gluons per unit area per unit rapidity of any hadrons including nuclei must increase rapidly as x decreases [14, 15].

The net-baryon number of relativistic heavy ion collisions is essentially transported by valence quarks that probe the saturation regime in the target by multiple scatterings. During relativistic heavy ion collisions, fast valence quarks in one nucleus scatter in another nucleus by exchanging soft gluons, leading to their redistribution in rapidity space. The valence quark parton distribution at large x is well known, which corresponds to the forward and backward rapidity region, to access the gluon distribution at small x in the target nucleus. Therefore, this picture provides a clean probe of the gluon distribution, $\varphi(x,p_{\rm T})$, at small x in the saturation regime.

For symmetric heavy ion collisions, the contribution of the fragmentation of the valence quarks in the projection is given by a simple formula for the rapidity distribution of interactions with a gluon in the target [14, 15]

$$\frac{\mathrm{d}N}{\mathrm{d}y} = \frac{C}{(2\pi)^2}\int \frac{\mathrm{d}^2 p_{\rm T}}{{p_{\rm T}}^2} x_1 q_{\rm v}(x_1)\varphi(x_2,p_{\rm T}), \tag{3}$$

here $x_1 q_{\rm v}(x_1)$ is the valence quark distribution of a nucleus, $\varphi(x_2, p_{\rm T})$ is the gluon distribution of another nucleus, $p_{\rm T}$ is the transverse momentum of the produced quark and y its rapidity. One important prediction of gluon saturation with geometric scaling is geometric scaling: the gluon distribution depends on x and $p_{\rm T}$ only through the scaling variable $p_{\rm T}^2/Q_{\rm s}^2(x)$, here $Q_{\rm s}^2(x) = A^{1/3}Q_0^2 x^{-\lambda}$. Geometric scaling was confirmed experimentally at HERA [1]. The fit value $\lambda = 0.2$–0.3 agrees with theoretical estimates based on next-to-leading order Balitskii-Fadin-Kuraev-Lipatov (BFKL) results [24–26].

The longitudinal momentum fractions carried, respectively, by the valence quark in the projectile and the soft gluon in the target are $x \equiv x_1 = (p_{\rm T}/\sqrt{s})\exp(y)$, and $x_2 = (p_{\rm T}/\sqrt{s})\exp(-y)$. Then we can deduce the relation as follows [14, 15]

$$x \equiv x_1,\ x_2 = x\mathrm{e}^{-2y},\ p_{\rm T}^2 = x^2 s\mathrm{e}^{-2y}. \tag{4}$$

The gluon distribution is defined as

$$\begin{aligned}\varphi(x_2,p_{\rm T}) &= \varphi\left(\frac{p_{\rm T}^2}{Q_{\rm s}^2(x_2)}\right)\\ &= 4\pi\cdot\frac{p_{\rm T}^2}{Q_{\rm s}^2(x_2)}\cdot\exp\left(-\frac{p_{\rm T}^2}{Q_{\rm s}^2(x_2)}\right).\end{aligned} \tag{5}$$

When we use the variables as Eq. (4), we can take the relation as follows

$$\frac{p_{\rm T}^2}{Q_{\rm s}^2(x_2)} = \frac{(x\cdot\sqrt{s}\cdot\mathrm{e}^{-y})^2}{A^{1/3}Q_0^2 x_2^{-\lambda}} = \frac{x^{2+\lambda}}{\mathrm{e}^{2(1+\lambda)y}}\cdot\frac{s}{Q_0^2}\cdot\frac{1}{A^{1/3}}. \tag{6}$$

If we make

$$\frac{p_{\rm T}^2}{Q_{\rm s}^2(x_2)} = x^{2+\lambda}\cdot\mathrm{e}^{\tau},$$

from Eq. (6) we can take

$$\mathrm{e}^{\tau}=\frac{1}{\mathrm{e}^{2(1+\lambda)y}}\cdot\frac{s}{Q_0^2}\cdot\frac{1}{A^{1/3}}, \tag{7}$$

and a geometrical scaling with rapidity is introduced as

$$\tau=\ln\left(\frac{s}{Q_0^2}\right)-\ln A^{1/3}-2(1+\lambda)y. \tag{8}$$

Thus Eq. (3) is given as follows

$$\frac{\mathrm{d}N}{\mathrm{d}y}=\frac{C}{2\pi}\int_0^1\frac{\mathrm{d}x}{x}xq_{\mathrm{v}}(x)\varphi(x^{2+\lambda},\ \mathrm{e}^{\tau}). \tag{9}$$

As mentioned before, the dependence of τ on y in Refs. [14, 15] is related to the peak position, but here we use the dependence of τ on y to define the rapidity limit of gluon saturation. A rapidity variable is introduced in Eq. (8) to discuss the gluon saturation rapidity region. The rapidity limit variable y is

$$y=\frac{1}{1+\lambda}(y_{\mathrm{b}}-\ln A^{1/6})+\frac{1}{2(1+\lambda)}\left(\ln\frac{m_{\mathrm{n}}^2}{Q_0^2}-\tau\right), \tag{10}$$

here $y_{\mathrm{b}}\approx\ln(\sqrt{s}/m_{\mathrm{n}})$ is the beam rapidity with nucleon mass m_{n}. It usually defines $x\leqslant 0.01$ as a small x region, and in this region, it is taken as the gluon saturation region. By taking $\tau=\ln(1/x)|_{x=0.01}$, we can figure out the rapidity region of gluon saturation as follows

$$y_{\mathrm{saturation}}=\frac{1}{1+\lambda}(y_{\mathrm{b}}-\ln A^{1/6})+\frac{1}{2(1+\lambda)}\left(\ln\frac{m_{\mathrm{n}}^2}{Q_0^2}-\tau\Big|_{x=0.01}\right). \tag{11}$$

The gluon distribution is

$$\varphi(x_2,p_{\mathrm{T}})=\begin{cases}\text{const} & (x<0.01)\\ 4\pi\dfrac{p_{\mathrm{T}}^2}{Q_{\mathrm{s}}^2(x_2)}\cdot\mathrm{e}^{-\frac{p_{\mathrm{T}}^2}{Q_{\mathrm{s}}^2(x_2)}}\cdot(1-x_2)^4 & (x>0.01)\end{cases}. \tag{12}$$

The valence quark distribution is

$$xq_{\mathrm{v}}(x)=\begin{cases}\propto\ x^{0.5} & (x<0.01)\\ \propto\ (xu_{\mathrm{v}}+xd_{\mathrm{v}}) & (x>0.01)\end{cases}. \tag{13}$$

So the net-baryon distribution which originates from the projectile is

$$\frac{\mathrm{d}N}{\mathrm{d}y}=\begin{cases}\propto\exp\left\{\dfrac{1+\lambda}{2+\lambda}y\right\} & (0\leqslant y\leqslant y_{\mathrm{saturation}})\\ \propto\displaystyle\int_{0.01}^1\frac{\mathrm{d}x}{x}(xu_{\mathrm{v}}+xd_{\mathrm{v}})4\pi\cdot\frac{p_{\mathrm{T}}^2}{Q_{\mathrm{s}}^2(x_2)} & \\ \cdot\exp\left\{-\dfrac{p_{\mathrm{T}}^2}{Q_{\mathrm{s}}^2(x_2)}\right\}\cdot(1-x_2)^4 & (y>y_{\mathrm{saturation}})\end{cases}. \tag{14}$$

The contribution of valence quarks in the other beam nucleus is added incoherently by changing $y\rightarrow -y$. The total rapidity distributions of the symmetry interaction systems are the summation of the contributions from the projectile and target, respectively

$$\left.\frac{\mathrm{d}N}{\mathrm{d}y}\right|_{\mathrm{total}}=\frac{\mathrm{d}N}{\mathrm{d}y}(y)+\frac{\mathrm{d}N}{\mathrm{d}y}(-y). \tag{15}$$

Compared with Refs. [14, 15], we will introduce effective dynamic quark mass in this paper by substituting the transverse momentum p_{T} as $\sqrt{(x\sqrt{s}\mathrm{e}^{-y})^2-m^2}$, i.e. $p_{\mathrm{T}}=\sqrt{(x\sqrt{s}\mathrm{e}^{-y})^2-m^2}$, here m is the dynamic quark mass, which was given by baryon mass in Refs. [14, 15]. The detailed study of dynamic mass with collision energies will be given in the next section.

3 The net baryon distributions in the SPS to LHC energy regions

Integrated net-proton rapidity distributions are scaled by a factor of 2.05 [2] to obtain net-baryon distributions. Rapidity distributions of net baryon for different energies of relativistic heavy nuclear collisions (Pb+Pb and Au+Au) at SPS and RHIC are given in Fig. 1.

The estimated numbers of participants are 390, 315, and 357 for $\sqrt{s_{\mathrm{NN}}}=17.3$, 62.4, and 200 GeV, respectively. The solid circles correspond to the experimental result of central collisions [3–9], and the real lines are the calculated results from the gluon saturation model with geometric scaling. It is found that our model describes the experimental data of net-baryon distributions very well when we discuss

Pb-Pb center collisions at the SPS energy region and Au-Au center collisions at the RHIC energy region. The $\lambda = 0.2$ and $Q_0^2 = 0.05$ GeV^2 are fixed in our whole calculation.

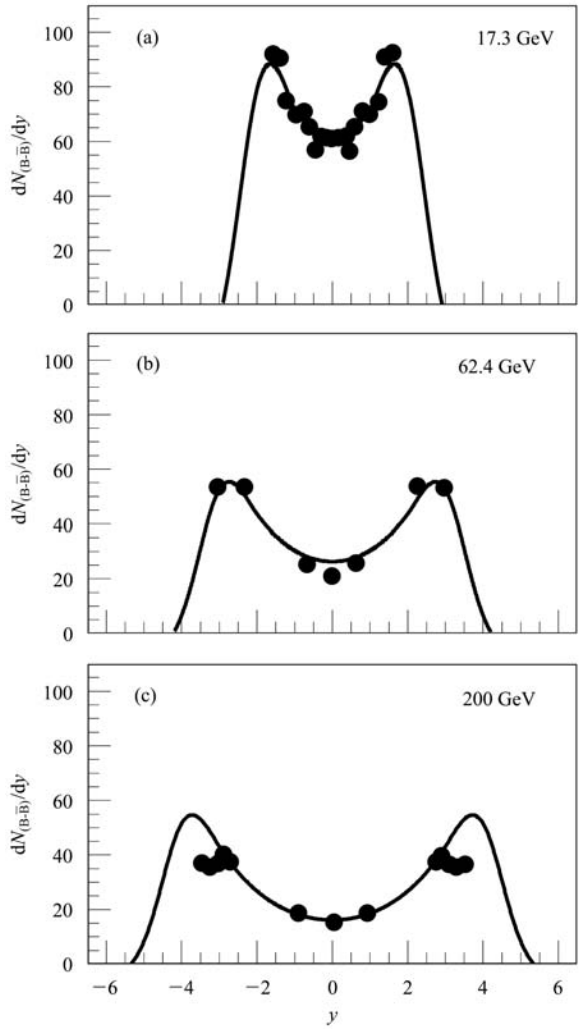

Fig. 1. Net-baryon distributions of central collisions at SPS $\sqrt{s_{\rm NN}} = 17.3$ GeV of Pb-Pb interactions and at RHIC $\sqrt{s_{\rm NN}} = 62.4$ and 200 GeV of Au-Au interactions; the experimental results are from Refs. [3–9].

We show in Fig. 2 the computation resulting from our discussions, the centrality dependence of the rapidity distribution at $\sqrt{s_{\rm NN}} = 200$ GeV. The estimated numbers of participants are 280, 200, 114 and 54 for centralities of 0–10%, 10%–20%, 20%–40%, and 40%–60% (from top to bottom) in Au+Au collisions at RHIC energies of $\sqrt{s_{\rm NN}} = 200$ GeV, respectively.

By comparing the experimental results with our model, we may get the conclusion for the net-baryon distribution from SPS to LHC as follows:

(1) The gluon saturation model with geometric scaling may be a good theory to study net-baryon distribution at central collisions at SPS and RHIC. The contributions of spectator nucleons can be neglected when considering only central collisions. The gluon saturation feature of central rapidity can be studied from our discussion. The values of central rapidity of gluon saturation ($y_{\rm saturation}$) are 1.06, 2.013 and 3.10 from Eq. (11) for $\sqrt{s_{\rm NN}} = 17.3$, 62.4, and 200 GeV, respectively.

(2) The net baryon rapidity distribution in central Pb+Pb collisions at LHC energies of $\sqrt{s_{\rm NN}} = 5.52$ TeV is predicted by the gluon saturation model with geometric scaling. The theoretical distribution is shown in Fig. 3 for $y_{\rm saturation} = 5.86$. The gluon saturation region is larger than those of RHIC and SPS. It is found that the separation of two symmetric peaks of net-baryon is much wider than that of SPS and RHIC.

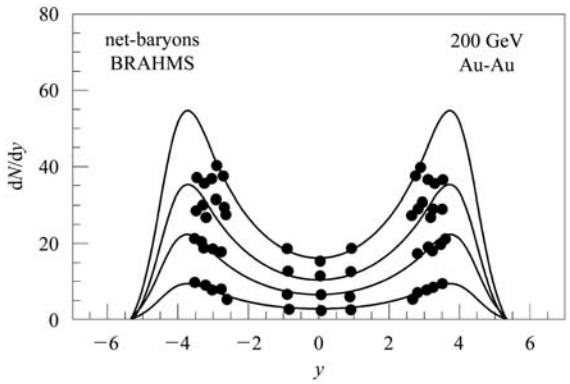

Fig. 2. Rapidity distributions of net baryons at different centrality; the experimental results are from Ref. [27], and the real lines are from our model.

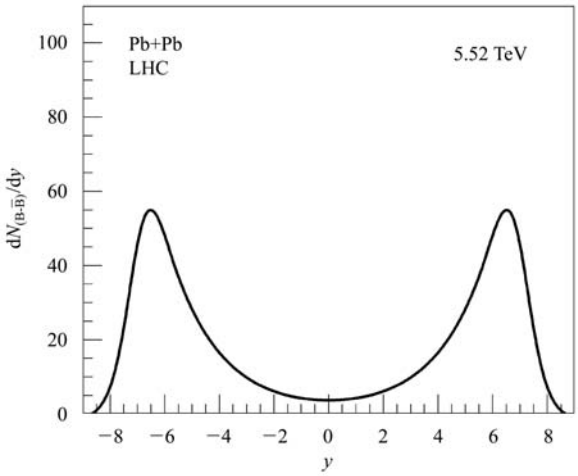

Fig. 3. The rapidity distribution of net-baryons in central Pb+Pb collisions at LHC energies of $\sqrt{s_{\rm NN}} = 5.52$ TeV. The theoretical distribution is from our discussion.

(3) The mean rapidity loss $\langle\delta y\rangle = y_{\rm b} - \langle y\rangle$ is shown in Fig. 4. We show that the dependence of mean rapidity loss increase on $y_{\rm b}$ as

$$\langle\delta y\rangle = 1.548\cdot\ln y_{\rm b} + 0.036. \tag{16}$$

In Fig. 4, the star ($*$) is our predicted result of the mean rapidity loss $\langle\delta y\rangle$ for Pb+Pb central collisions at LHC energies of $\sqrt{s_{\rm NN}} = 5.52$ TeV ($y_{\rm b} = 8.68$). In high-energy central nucleus-nucleus collisions, baryon matter will be slowed down and will lose a few units of rapidity. The term "nuclear stopping power" was introduced in high-energy nucleus-nucleus collisions by Busza and Goldhaber to refer to the degree of stopping an incident nucleon suffers when it impinges on the nuclear matter of another nucleus. Usually the mean rapidity loss $\langle\delta y\rangle = y_{\rm b} - \langle y\rangle$ was used to represent the nuclear stopping power of nucleus-nucleus collisions.

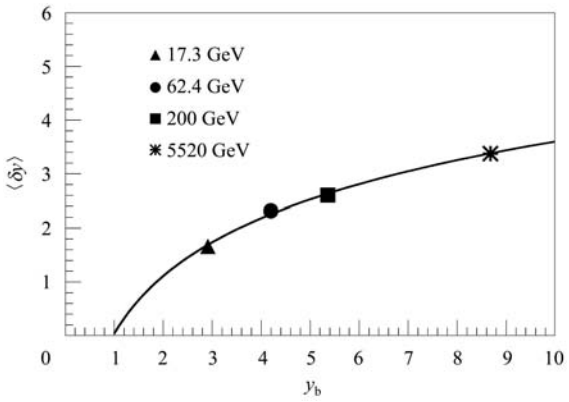

Fig. 4. The dependence of mean rapidity loss $\langle\delta y\rangle$ on beam rapidity $y_{\rm b}$. The ▲, ●, ■, $*$ are the calculated results from our discussion for $\sqrt{s_{\rm NN}} = 17.3$, 62.4, 200 and 5520 GeV, respectively. The real curve is the fit curve with $\langle\delta y\rangle = 1.548\cdot\ln y_{\rm b} + 0.036$.

(4) It is shown in Fig. 5 that the dependence of percentage ratios of the net-baryon production from the central gluon saturation region on incident energy at $\sqrt{s_{\rm NN}} = 17.3$, 62.4 , 200 and 5520 GeV. It is found that the percentage ratio from the central gluon saturation region increases with the increase of the colliding energies. The percentage ratio from the saturation region rises rapidly from SPS $\sqrt{s_{\rm NN}} = 17.3$ GeV to RHIC $\sqrt{s_{\rm NN}} = 62.4$ GeV, but slowly from RHIC $\sqrt{s_{\rm NN}} = 200$ GeV to LHC $\sqrt{s_{\rm NN}} = 5520$ GeV. It is found that the percentage ratio is 43.17% at $\sqrt{s_{\rm NN}} =$ 17.3 GeV, but 56.31% at $\sqrt{s_{\rm NN}} = 5520$ GeV. It seems that more than half of the net baryon at the LHC comes from the central gluon saturation region.

(5) The dependence of the effective quark mass $m_{\rm q}$ on incident projective rapidity in the CMS at $\sqrt{s_{\rm NN}} = 17.3$, 62.4, 200 and 5520 GeV is shown in Fig. 6. It is found that the effective quark mass $m_{\rm q}$ varies slowly with the varying of the incident energies, and $m_{\rm q}$ varies between 0.24 and 0.26.

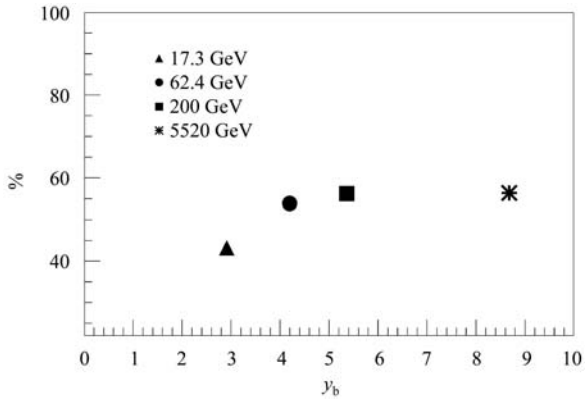

Fig. 5. The dependence of the percentage of net-baryon from the central gluon saturation region on the colliding energies at $\sqrt{s_{\rm NN}} =$ 17.3, 62.4, 200 and 5520 GeV.

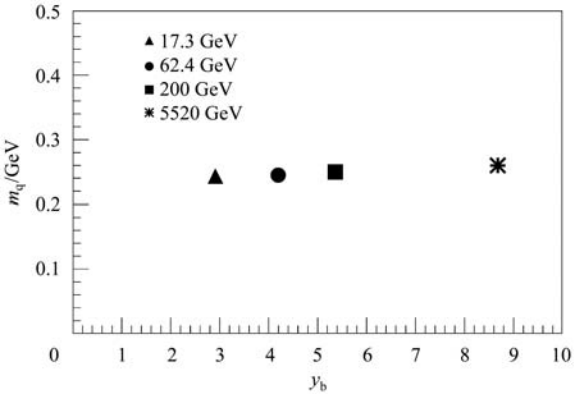

Fig. 6. The dependence of the effective quark mass on incident projective rapidity in the CMS at $\sqrt{s_{\rm NN}} = 17.3$, 62.4, 200 and 5520 GeV.

4 Summary and conclusion

As discussed in Refs. [14, 15], two distinct and symmetric peaks with respect to rapidity y occur at SPS energies and beyond in A+A collisions. A geometrical scaling feature of the peak position of net baryon rapidity distributions was proposed to discuss the net-baryon distribution [14, 15]. The rapidity separation between the peaks increases with energy and decreases with increasing mass number, A, reflecting larger baryon stopping for heavier nuclei, as was investigated phenomenologically in the Non-uniform Flow Model (NUFM) [10–13]. In this work we show geometrical scaling with a gluon saturation rapidity

limit, and also discuss the net-baryon rapidity distribution feature in the SPS，RHIC and LHC.

A saturation model for net-baryon distributions that successfully describes the net-baryon rapidity distributions and their energy dependence is presented in this paper. The remarkable feature of geometric scaling predicted by our discussion is reflected in the net-baryon rapidity distribution, providing a direct test of gluon saturation rapidity and x regions. The gluon saturation model is proposed by introducing a rapidity variable with a gluon saturation region to define the gluon saturation region of the central rapidity region of centrally colliding heavy ions at ultra-relativistic energies.

The gluon saturation features of central rapidity at SPS and RHIC can be investigated. It is found that the values of central rapidity of the gluon saturation region increase with colliding energy. The detailed dependence of rapidity ($y_{\rm saturation}$) of the central gluon saturation on colliding energy is also investigated in this paper. We also predict the net baryon rapidity distribution in central Pb+Pb collisions at LHC energies of $\sqrt{s_{\rm NN}}=5.52$ TeV using the gluon saturation model with geometric scaling. The gluon saturation region is larger than those of RHIC and SPS, and the separation of two symmetric peaks of net-baryon is much wider than that of SPS and RHIC.

It is shown that the gluon saturation feature is an important feature with increasing colliding energy. It seems that more than half of the produced net baryon numbers (56.31%) at the LHC come from the central gluon saturation region, but the percentage ratio is 43.17% at SPS $\sqrt{s_{\rm NN}}=17.3$ GeV.

The dependencies of the percentage of net-baryon from the central gluon saturation region and stopping power on colliding energies are also studied in this paper. It is also found that the mean rapidity loss shows a linear dependence on $\ln y_{\rm b}$. From that we can predict the mean rapidity loss for future LHC experimental data.

References

1 Breitweg J et al. Eur. Phys. J. C, 1999, **7**: 609
2 Iancu E, McLerran M. Phys. Lett. B, 2001, **510**: 145
3 Arsene I C et al. Phys. Lett. B, 2009, **677**: 267
4 Bearden I G et al. Phys. Rev. Lett., 2004, **93**: 102301
5 Klay J L et al. Phys. Rev. Lett., 2002, **88**: 102301
6 Bearden I G et al. Phys. Rev. Lett., 2005, **94**: 162301
7 Barrette J et al. Phys. Rev. C, 2000, **62**: 024901
8 Ahle L et al. Phys. Rev. C, 1999, **60**: 064901
9 Appelshauser H et al. Phys. Rev. Lett., 1999, **82**: 2471
10 FENG Sheng-Qin, LIU Feng, LIU Lian-Shou. Phys. Rev. C, 2000, **63**: 014901
11 FENG Sheng-Qin, YUAN Xian-Bao, SHI Ya-Fei. Modern Phys. Lett. A, 2006, **21**: 663
12 FENG Sheng-Qin, XIONG Wei. Phys. Rev. C, 2008, **77**: 044906
13 FENG Sheng-Qin, YUAN Xian-Bao. Science in China Series G, 2009, **52**: 198
14 Mehtar-Tani Y et al. Phys. Rev. C, 2009, **80**: 054905
15 Mehtar-Tani Y et al. Phys. Rev. Lett., 2009, **102**: 182301
16 Gribov L V et al. Phys. Rep., 1983, **100**: 1
17 Mueller A H, QIU J W. Nucl. Phys. B, 1986, **268**: 427
18 McLerran L, Venugopalan R. Phys. Rev. D, 1994, **50**: 2225
19 Kharzeev D et al. Nucl. Phys. A, 2005, **747**: 60
20 Kharzeev D, Levin E. Phys. Lett. B, 2001, **523**: 79
21 Kharzeev D et al. Phys. Lett. B, 2004, **599**: 23
22 Baier R et al. Nucl. Phys. A., 2006, **764**: 515
23 Triantafyllopoulos D N. Nucl. Phys. B, 2003, **648**: 293
24 Kuraev E A et al. Sov. Phys. JETP, 1977, **45**: 199
25 Ya. Ya. Balitsky et al. Sov. J. Nucl. Phys, 1978, **28**: 822
26 Lipatov L N. Sov. J. Nucl. Phys. 1976, **23**: 338
27 Debbe R et al. J. Phys.G. 2008, **35**: 104004